Surface Modification of Cellulose Nanofibrils for Poly(lactic acid) Composite Application

Ping Qu, Yitong Zhou, Xiaoli Zhang, Siyu Yao, Liping Zhang

College of Material Science and Technology, Beijing Forestry University, Beijing 100083, People's Republic of China

Received 9 July 2011; accepted 12 October 2011
DOI 10.1002/app.36360
Published online 1 February 2012 in Wiley Online Library (wileyonlinelibrary.com).

ABSTRACT: 3-Methacryloxypropyltrimethoxysilane (MEMO) was used to modify the surface of cellulose nanofibrils (CNF) to improve the interfacial adhesion between the hydrophilic CNF and the hydrophobic poly(lactic acid) (PLA). MEMO modified CNF (M-CNF) were characterized by means of Fourier transform infrared spectroscopy (FTIR), thermo gravimetric analysis (TGA), and atomic force microscope (AFM). Testing thin films with good transparency were obtained by casting the DMAC solutions of the composites onto glass plates and evaporating the solvent at 80°C. PLA/M-CNF composites were tested by tensile testing, scanning electron microscope (SEM), and AFM. The effect of MEMO and CNF on performance of PLA was investigated. The FTIR analysis successfully showed that coupling reaction has been successfully occurred and the hydroxyl groups of MEMO are strongly hydrogen bonded to that of CNF. The thermal stability of M-CNF was little decreased. The M-CNF kept their morphological integrity. The highest tensile strength of composites was obtained for PLA with 1.0% v/v MEMO and 1.0 wt % CNF. M-CNF disperse well and cross with each other in the PLA matrix. © 2012 Wiley Periodicals, Inc. J Appl Polym Sci 125: 3084–3091, 2012

Key words: cellulose nanofibrils; poly(lactic acid); nanocomposites; modification; compatibility

INTRODUCTION

Because of the biodegradability and recyclability, biopolymers are attractive materials. They can replace the conventional petroleum-based packaging materials in respect of energy resources and environmental pollution. Poly(lactic acid) (PLA) is one of most important biopolymers made from the renewable resources such as corn, beet sugar, and so on.[1–5] PLA is an enantiomeric polyester including poly(L-lactic acid) (PLLA) and poly(D-lactic acid) (PDLA). The chiral center in the structure allows varied enantiomeric compositions of PLA.[6] With good processability, biodegradability, and recyclability, PLA was regarded as one of the most promising polymer and was expected to substitute some of the non-biodegradable plastics.[7,8] PLA shows good potential for applications in packaging and in the automotive and biomedical fields.[9] However, mechanical and thermal properties of PLA are inferior to those of conventional petroleum-based polymers.[9–11] To improve the properties of PLA it is desirable to combine PLA with reinforcing elements. Cellulose nanofibrils (CNF) have many advantages, such as good mechanical properties (e.g., Young's modulus of about 150 GPa),[12,13] renewability, sustainability, availability, low density, biodegradability, and last but not least, low cost, which offer greater opportunities to develop a new class of light weight, transparent, and environmental friendly nanocomposites.

One disadvantage of CNF for their application in polyester is the strong hydrophilic nature due to large amount of hydroxyl groups, which causes a weak interface and reduce the mechanical properties of the composites. To improve their compatibility, two routes have been investigated, one is coating surface of the fibrils with surfactants having polar heads and long hydrophobic tails, the other is grafting hydrophobic chains at the surface of the cellulose fibrils. CNF have been treated with surfactants,[14] compatibilizer, or chemicals.[15–20] However, there have been few reports on the surface modification of CNF by 3-methacryloxypropyltrimethoxysilane (MEMO) for PLA composite application.

In this article, MEMO was used to modify the surface of CNF and then the modified CNF (M-CNF) were added into PLA as reinforced phase. The effect of MEMO and the addition of CNF on the properties of PLA matrix were investigated. The structures, morphology, and thermal stability of modified CNF were characterized. The surface morphology of M-CNF/PLA composites was detected by atomic

Correspondence to: L. Zhang (zhanglp418@163.com).
Contract grant sponsor: Specific Programs in Graduate Science and Technology Innovation of Beijing Forestry University; contract grant number: BLYJ201105.
Contract grant sponsor: Beijing Natural Science Foundation; contract grant number: 2112031.

© 2012 Wiley Periodicals, Inc.

force microscope (AFM). Mechanical properties and microscopy of the fracture surfaces of composites were also presented in this article.

EXPERIMENTAL

Materials

PLA (M_w = 100,000, purchased from Shanghai Yisheng industry Ltd., Shanghai, China) was used as the matrix. Bleaching wood pulp was purchased from a pulp and paper mill in Shandong province, China. MEMO that was used to modify the surface of CNF purchased from Beijing shenda fine chemical Co., Ltd. The solvents *N*,*N*-dimethylacetamide (DMAC) and sulfuric acid (98%) were purchased from Shantou Xilong Chemical Plant and Beijing Chemical Plant, respectively.

Preparation of nanocomposites

Surface modification of cellulose nanofibrils

The pulpboard was pretreated with 15% diluted sulfuric acid at 80°C for 4 h at mixing speed of 200 rpm (the solid to liquid ratio is 1 : 20). After thorough washing with deionized water by filtration to remove the H^+ and SO_4^{2-}, the cake was immersed into 95% ethylalcohol (the solid to liquid ratio is 1 : 100). The suspension was then homogenized at a high pressure of 100 MPa for three times (GEA Niro Soavi, Italy). The CNF dispersing in ethanol (1.0 wt %) was obtained.[15] Acetic acid was added to adjust the pH of solution to 4–5. Then MEMO was added into CNF ethylalcohol suspension to yield final concentrations of 0.5, 1.0, 1.5, and 2.0% v/v. The suspension was stirred for 1 h at room temperature. The CNF was washed twice with ethanol after modification, and then washed several times with DMAC in order to remove any physical deposition of modifier on CNF.

PLA/MEMO-cellulose nanofibrils composites preparation

The desired amount of PLA was added into MEMO-CNF (designated M-CNF) suspension, ultrasonicated for 15 min (KQ 5200DB, China) and then stirred at 80°C for 4 h. The suspension was poured onto a glass and scraped. The composites were cured at 80°C for 5–10 min and postcured under vacuum condition at 80°C for 12 h to ensure that the solvent had completely evaporated. The thickness of films was approximately 80 μm.

Performance and characterization of materials

FTIR characterization

Fourier transform infrared spectroscopy (FTIR) spectrum of the CNF and M-CNF were obtained with dried powdered samples on a Tensor 27 (Bruker, Germany) device in the range of 4000–400 cm^{-1}. KBr pellets were made on a hydraulic press of a mixture of the samples and KBr powder (1 : 100 in weight). Thirty-two scans were accumulated at a resolution of 2 cm^{-1}.

TGA analysis

The thermal stability was assessed with thermo gravimetric analysis (TGA) carried out on a SHIMADZU TGA-60. Temperature range was from ambient temperature to 600°C at a heating rate of 20 °C/min. α-Al_2O_3 was taken as the reference material. These tests were carried out under nitrogen atmosphere (20 mL/min) in order to prevent thermoxidative degradations.

Atomic force microscope

The M-CNF and M-CNF/PLA composites were characterized using a SHIMADZU SPM 9600 scanning probe microscope. Images were collected with a constant force mode. For the CNF analysis, a droplet of the DMAC suspension of 0.1% M-CNF was dried on a mica surface prior to AFM examination.

Mechanical tests

Testing was conducted on a DCP-KZ300 at a crosshead speed of 20 mm/min. Samples for mechanical analysis were prepared with dimensions of approximately 15 mm × 100 mm. Five measurements were made for each specimens, and the average value was take as the datum point.

Scanning electron microscope

The fracture surfaces of 1.0% v/v MEMO/1.0 wt % CNF/PLA composites, 0.5% v/v MEMO/1.0 wt % CNF/PLA composites, and 1.0% v/v MEMO/0.5 wt % CNF/PLA composites were studied with a JSM 5900 scanning electron microscope (SEM) under an accelerating voltage of 5 kV. All the surfaces were sputtered with gold.

RESULTS AND DISCUSSION

Surface modification of cellulose nanofibrils

The reaction involves the hydrolysis of —O—CH_3 (Figure 1a) and condensation of —Si—OH (Figure 1b) which forms —Si—O—Si— bearing oligomers. The oligomers can form hydrogen bonds with —OH groups of cellulose at room temperature (Figure 1c). Y: CH_2=C(CH_3)COO$CH_2CH_2CH_2$.

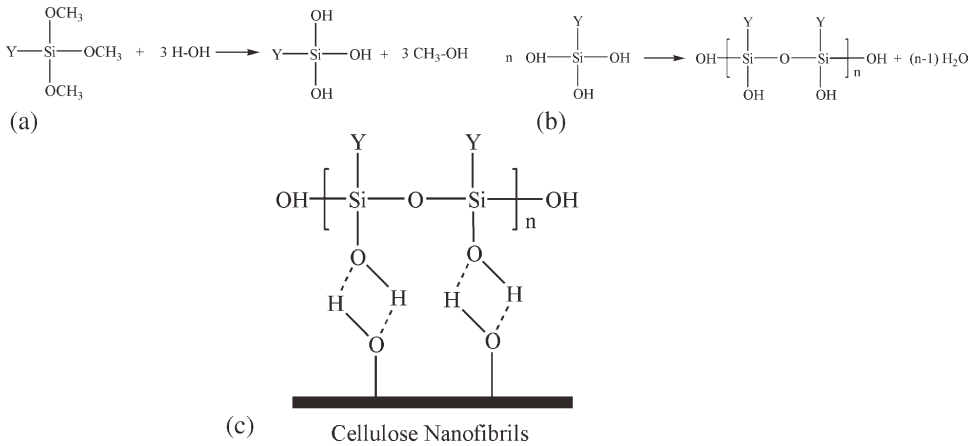

Figure 1 The reaction mechanism of MEMO on the cellulose surface. (a) Hydrolysis reaction; (b) condensation reaction; (c) hydrogen bonds formed between CNF and MEMO.

FTIR characterization

Figure 2 shows the FTIR spectra of CNF and M-CNF. From the spectrum of CNF, it can be observed that the hydrogen bonded —OH stretching is located at 3600–3200 cm^{-1}, the C—H stretching at 2900 cm^{-1}, the OH bending of adsorbed water at 1635 cm^{-1}, the $-CH_2$ bending situates at 1432 cm^{-1}, and the C—H bending at 1371 cm^{-1}, which represent characteristic peaks of CNF. The peak at 1061 cm^{-1} is related to the C—O stretching. The C—H bending and $-CH_2$ stretching are observed at 896 cm^{-1}.[21]

The spectrum of CNF treated with MEMO after drying at 80°C for 1 day shows the bond at 3600–3200 cm^{-1} which is sharper than that of CNF. The reason maybe that the hydroxyl groups of MEMO are strongly hydrogen bonded to that of CNF as shown in Figure 1.[22,23] And some MEMO also can form intramolecular hydrogen bonding among its own chains. The strong absorption of the cellulose bond in the region of 1000–1200 cm^{-1} makes it difficult to completely assign the Si—O—Si and Si—O—$C_{cellulose}$.[24] Because of the overlap of Si—O—Si bond and the C—O stretching of cellulose, the peaks of M-CNF are increased, further evidence of silane adsorption.[21] The strong absorption at 1720 cm^{-1} and 1640 cm^{-1} belong to the characteristic peak of C=O and C=C, respectively. It can be seen that coupling reaction has been occurred between MEMO and CNF.

TGA analysis

Figure 3 shows the TGA and DTA curves of the CNF and CNF treated with MEMO. The CNF exhibits higher thermal stability than the M-CNF. As shown in Figure 3, the onset temperature of the decomposition for CNF and M-CNF are nearly the same, but the extensional onset temperature of the decomposition for CNF and M-CNF are different. The extensional onset temperature of the decomposition of CNF is 330.54°C compared to 321.56°C of M-CNF. DTA is the first derivative of weight loss. From the DTA curves in Figure 3, it can be seen that the maximum reaction rate of M-CNF, the peak of DTA curves, is 349.61°C compared to 361.02°C of CNF. It is because that the thermal stability of

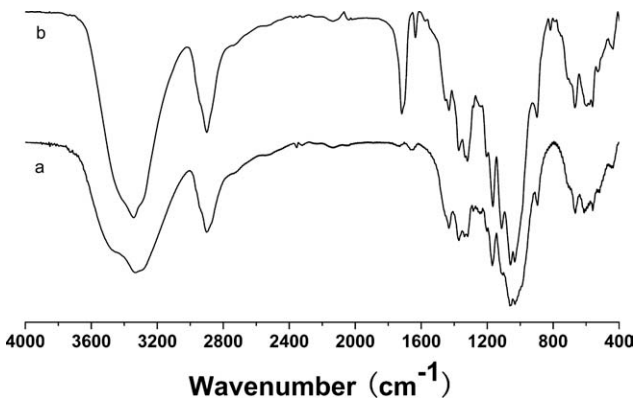

Figure 2 FTIR spectra of CNF (a) and M-CNF (b).

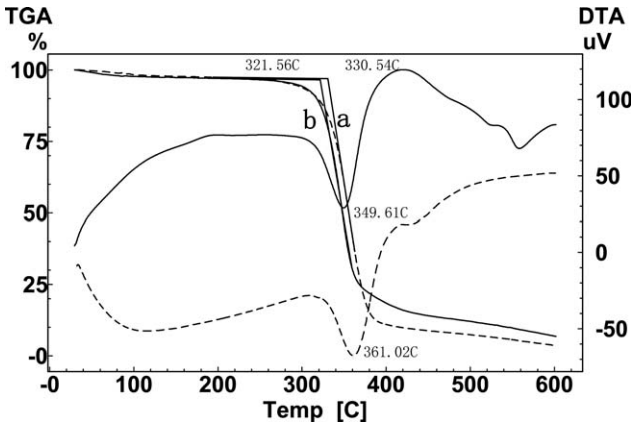

Figure 3 Thermal stability of CNF (a) and M-CNF (b).

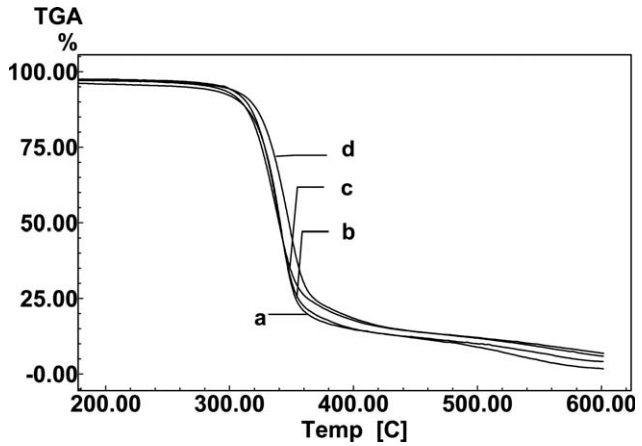

Figure 4 Thermal stability of different modification degrees of CNF. (a) 0.5 v/v % MEMO modified CNF; (b) 1.0 v/v % MEMO modified CNF; (c) 1.5 v/v % MEMO modified CNF; (d) 2.0 v/v % MEMO modified CNF.

M-CNF is poorer than pure CNF and decomposes at a lower temperature. When the temperature exceeds 371°C, the residue of M-CNF is more than that of CNF, which may be the Si that cannot undergo thermal decomposition.

Figure 4 shows the different modification degrees of CNF by MEMO, 0.5, 1.0, 1.5, and 2.0% v/v, respectively. There is only a little difference among onset temperature of the decomposition of the different modification degrees of CNF. Modification degrees of 2.0% v/v for CNF have the most residue and 0.5% v/v for CNF have the least. High values of modification degrees have more residues that ascribe to Si. The degree of substitution can be characterized by the content of Si. The degree of substitution of a, b, c, and d is 2.05%, 3.84%, 5.90%, and 6.84%, respectively.

Morphology of the M-CNF

During scanning, the amplitude of the oscillating cantilever is maintained at a set point value Asp by altering the vertical position of the sample, and changes in the vertical position are presented as a height image. Phase imaging refers to the mapping of the phase lag between the signal that drives the cantilever oscillation and the cantilever oscillation output signal. Changes in the phase lag reflect changes in the mechanical properties of the sample surface. The phase lag is monitored while the topographic image is being taken so that images of topography and material properties can be collected simultaneously.

Morphology of M-CNF was characterized by AFM, as shown in Figure 5 which corresponds to untreated CNF.[15] Height image of M-CNF is blurred, not clear, because of the existence of MEMO reaction with CNF. However, from the phase mode image, it can distinguish the skeleton of CNF from the surface MEMO. Also, the result is consistent with the FTIR and TGA that the MEMO coupling agent is successfully grafted on MFC. With the present reaction condition, destruction of CNF morphology is not observed. The M-CNF keeps their integrity and rod-like morphology, which can be used as the reinforcing materials in polyester.

Picture of the M-CNF dispersing in DMAC

Figure 6 presents suspensions of different degrees of modification of CNF with MEMO after letting it rest

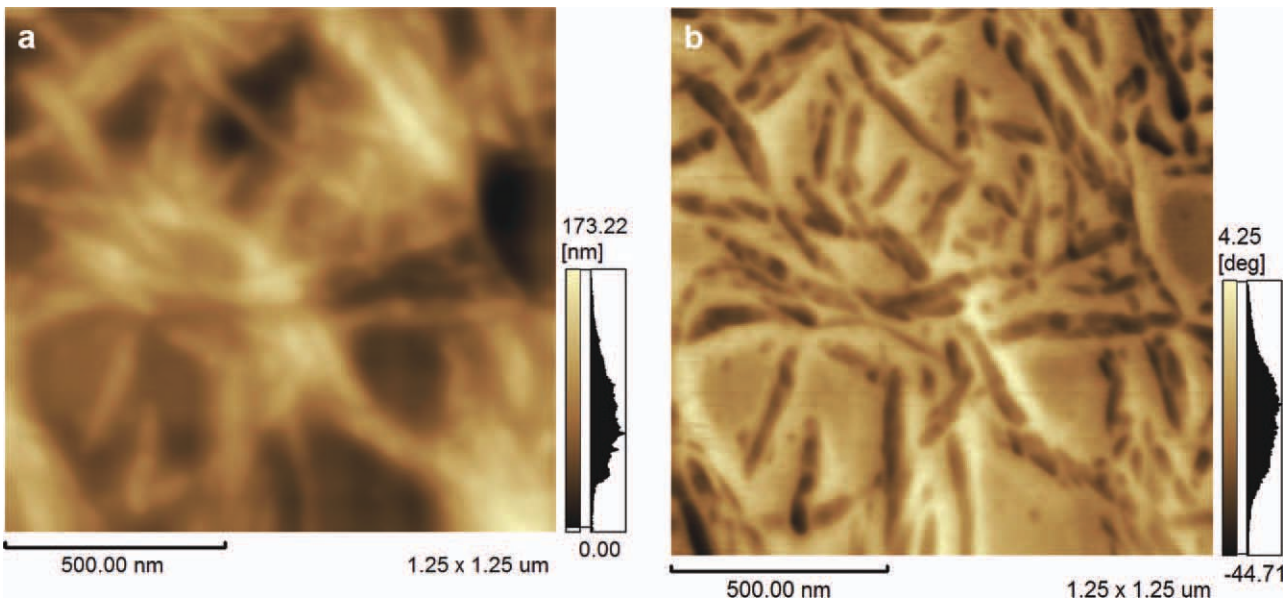

Figure 5 AFM images of M-CNF, collected simultaneously. Field of view 1.25 μm × 1.25 μm. (a) Height image; (b) phase image. [Color figure can be viewed in the online issue, which is available at wileyonlinelibrary.com.]

Figure 6 Picture of suspensions of different modification degrees of CNF in DMAC. (a) 0.5 v/v % MEMO modified CNF, phase separated suspension with more deposition; (b) 1.0 v/v % MEMO modified CNF, phase separated suspension with less deposition; (c) 1.5 v/v % MEMO modified CNF, well-dispersing suspension; (d) 2.0 v/v % MEMO modified CNF, well-dispersing suspension. [Color figure can be viewed in the online issue, which is available at wileyonlinelibrary.com.]

for at least a week (in the same concentration, 0.02 g/mL). Different behaviors can be observed for the suspensions in DMAC. The 1.5% v/v, 2.0 v/v% M-CNF can be homogeneously dispersed in DMAC at ambient temperature. However, in 0.5, 1.0% v/v M-CNF can be seen the flocculation and total separations have occurred. The higher the filler concentration was, the more hydroxyl groups of CNF reacted with MEMO. The more hydrophilic group turned into hydrophobic group. The more the hydrophobic M-CNF the better dispersions in DMAC. From Figure 6, the conclusion we can get is different surface modification of CNF are produced.

Mechanical tests

The mechanical behavior for films of the composites reinforced with 0.25, 0.5, 1.0, 1.5, and 2.0 wt % of 1.0% v/v MEMO modified CNF was performed by tensile testing at room temperature. Figure 7 shows the effects of M-CNF content on the tensile strength and elongation. The M-CNF/PLA composites present a change in the properties as the M-CNF concentration increases. The mechanical properties of composites with M-CNF content lower than 0.5% and higher than 1.5% are poorer. But the composites shows enhanced mechanical properties in comparison with the neat PLA (39 MPa) (Qu et al. 2010). By incorporating 1.0% M-CNF, composites have the highest tensile strength and elongation, increased by 42.3% and 28.2% compared to pure PLA. When M-CNF content is lower than 0.5%, there is not enough M-CNF to cross with each other and become a network in the PLA matrix. But, too much M-CNF in the PLA matrix can cause aggregates which weaken the interfacial adhesion between M-CNF and PLA matrix. The elongation shows the same trend with tensile strength. As a consequence of the aggregates in the composites, zones with accentuated fragility are created, which lead to a brittleness in this material.[25]

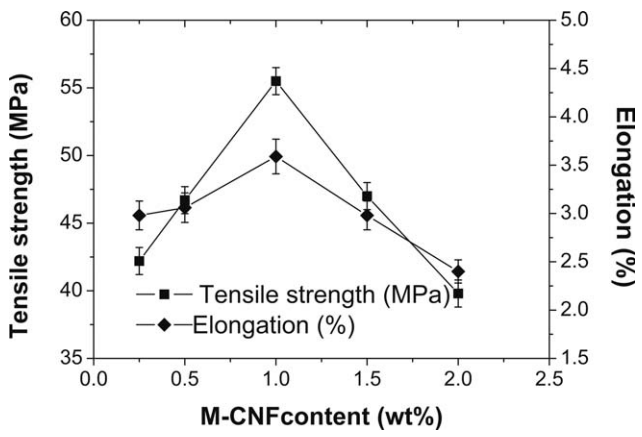

Figure 7 M-CNF content on mechanical properties of composites.

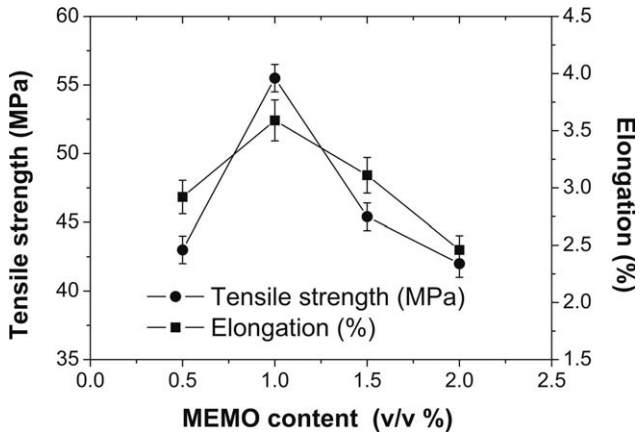

Figure 8 MEMO content on mechanical properties of composites.

It is known that the filler plays an important role in determining the mechanical properties of MEMO modified CNF/PLA composites. One of the main factors that affect the mechanical properties of CNF-reinforced material is the CNF–matrix interfacial adhesion. A weak interfacial region will reduce the efficiency of stress transfer from the matrix to the reinforcement component and low strength can be anticipated.[26] So the mechanical properties of composites are not only determined by the content of CNF but also by the content of the MEMO. The more MEMO added, the thicker MEMO that cover the CNF surface is gained. Figure 8 shows the effect of MEMO content on mechanical properties of composites when the content of CNF was 1.0 wt %.

The tensile results indicate that the addition of MEMO can promote the reinforcement of CNF/PLA composites. And the mechanical properties of composites with content higher than 1.5% or lower than

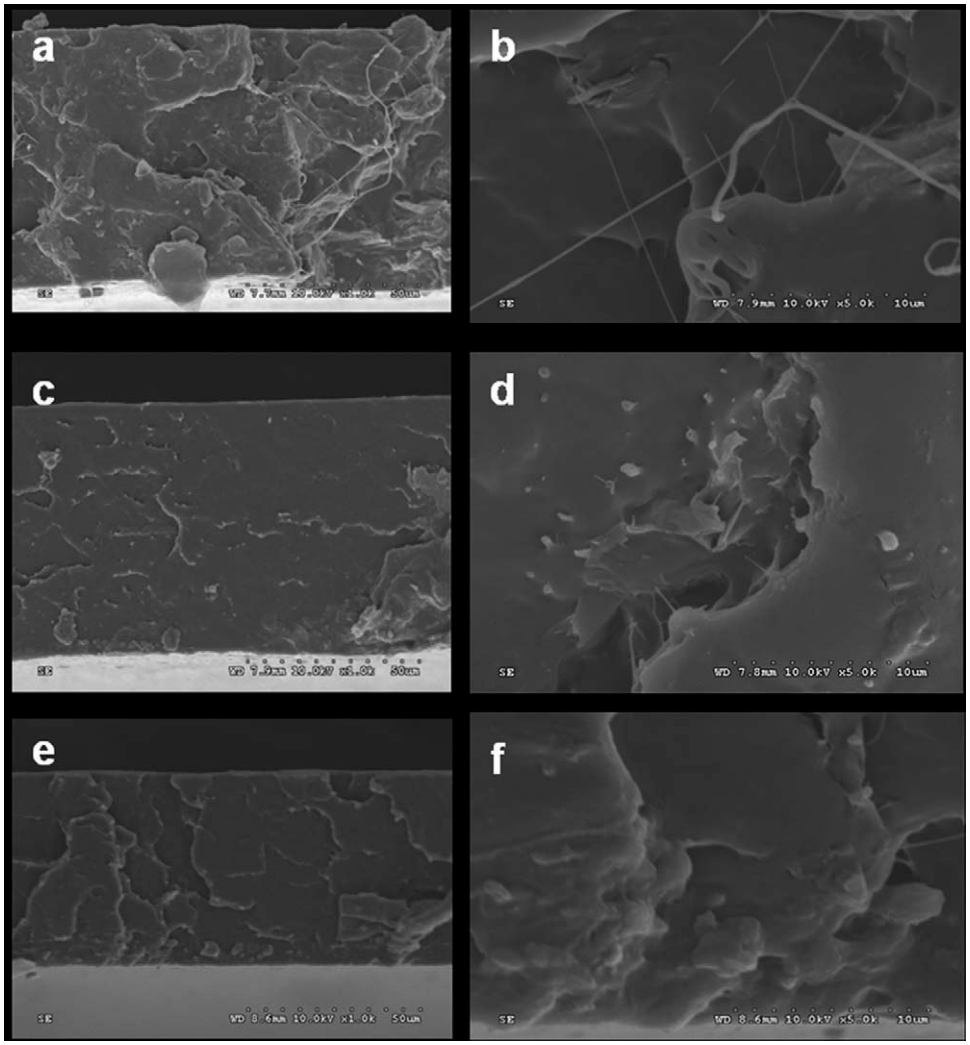

Figure 9 Scanning electron micrograph (SEM) photos of the fracture surfaces of the composites. (a,b) 1.0 v/v % MEMO/1.0 wt % CNF/PLA composites, (a): ×1000; (b): ×5000; (c,d): 0.5 v/v % MEMO/1.0 wt % CNF/PLA composites, (c): ×1000; (d): ×5000; (e,f): 1.0 v/v % MEMO/0.5 wt % CNF/PLA composites, (e): ×1000; (f): ×5000.

0.5% are poorer than the content of 1.0%. The tensile strength of composites firstly increases and then decreases with the MEMO content increasing. The reason may be that the lower the content the fewer the MEMO cover on the surface of CNF and the MEMO cannot form enough interfacial layer to join the hydrophilic CNF and hydrophobic PLA. More MEMO undergoes self-condensation and form hydroxyl bond among MEMO, which make the layer between PLA and CNF too thick and lead to the conclusion that there are very little stress-transfer properties in those materials.

Scanning electron microscope analysis

The PLA and M-CNF are low in contrast under high energy electron beam, so the dispersion conditions of M-CNF in PLA matrix cannot be seen. The SEM analysis has been performed in order to investigate the fracture mode of the composites. The micrographs have been taken on the tensile fracture surface. From Figure 9(a), the tough characteristics are demonstrated with a rough fracture surface severely deformed PLA matrix. And upon high magnification [Fig. 9(b)], some drawn deformation and wire drawing phenomenon are seen. Thus, the tensile behavior of the 1.0% v/v MEMO/1.0 wt % CNF/PLA composites should attribute to the non-brittle failure. When the MEMO content decreases to 0.5% [Fig. 9(c)], a typical morphology of semi-brittle failure with less rough surface is seen. In Figure 9(d), the drawn deformation and wire drawing phenomenon are less compared to Figure 9(b) due to the decrease of MEMO content. There is only roughness and no wire drawing phenomenon can be seen in Figure 9(e,f). It is because the M-CNF content is too lower to form network. From the SEM results, we can get the conclusion that both CNF and MEMO play an

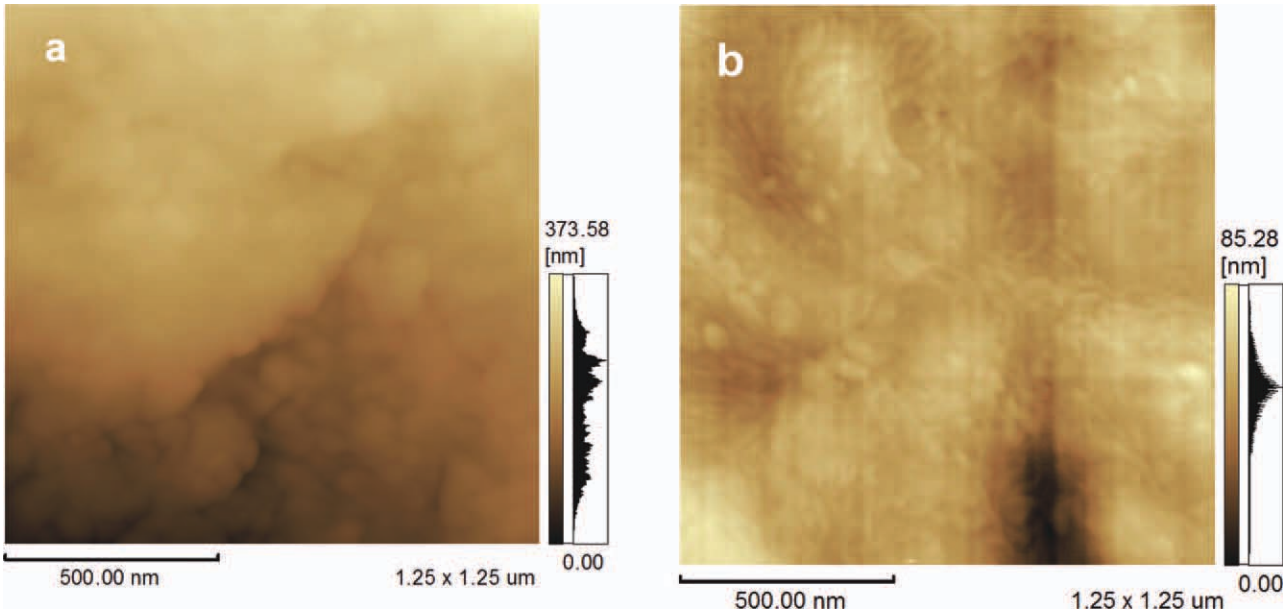

Figure 10 The AFM images of the surface morphology of PLA (a) and M-CNF/PLA composites (b), Field of view 1.25 μm × 1.25 μm. [Color figure can be viewed in the online issue, which is available at wileyonlinelibrary.com.]

important role in improving the performance of PLA.

Morphology of nanocomposites

Figure 10 shows the surface of the pure PLA and the composites 1.0% v/v MEMO/1.0 wt % CNF observed by AFM. The M-CNF in the composites was coated by PLA molecular, which greatly affect the detection of the morphology of M-CNF dispersing in the PLA matrix. To avoid this, the pure PLA and M-CNF/PLA composites were immersed in water for a week at 37°C to make the surface PLA degradation and exposed the M-CNF dispersing in the PLA matrix. It can be seen that CNF disperse well and cross with each other in the PLA matrix. In the field of view 1.25 μm × 1.25 μm, aggregation of M-CNF cannot be observed.

CONCLUSIONS

From the spectrum of CNF and M-CNF, we get the conclusion that coupling reaction has been successfully occurred between MEMO and CNF. The reaction mechanism of MEMO on the cellulose surface is presented. The M-CNF has a less thermal stability than CNF because the thermal stability of MEMO modifier is poorer than pure CNF and decomposes at a lower temperature. The more residue of M-CNF than that of CNF belongs to Si that cannot undergo thermal decomposition. The CNF modified with MEMO keep their integrity and rod-like morphology, which can be used as the reinforcing materials in polyester, such as PLA, from height and phase image of AFM. It is noticed that the tensile strength and elongation of the samples first increases and then decreases with the M-CNF or MEMO content increasing. The highest tensile strength of composites is obtained for PLA with 1.0% v/v MEMO and 1.0 wt % CNF. These SEM observations confirm the tensile results. Both CNF and MEMO play an important role in improving the performance of PLA. In the field of view 1.25 μm × 1.25 μm, M-CNF disperse well in the PLA matrix.

References

1. Nijenhuis, A. J.; Gripma, D. W.; Pennings, A. J. Macromolecules 1992, 25, 6419.
2. Tsuji, H.; Daimon, H.; Fujie, K. Biomacromolecules 2003, 4, 835.
3. Vink, E. T. H.; Rábag, K. R.; Glassner, D. A.; Gruber, P. R. Polym Degrad Stab 2003, 80, 403.
4. Yang, S. L.; Wu, Z. H.; Yang, W.; Yang, M. B. Polym Test 2008, 27, 957.
5. Lee, S. H.; Wang, S. Q.; Teramoto, Y. J Appl Polym Sci 2008, 108, 870.
6. Kale, G.; Auras, R.; Singh, S. P.; Narayan, R. Polym Test 2007, 26, 1049.
7. Garlotta, D.; Literature, A. J Polym Environ 2002, 9, 63.
8. Liu, D. Y.; Yuan, X. W.; Bhattacharyya1, D.; Easteal, A. J. Expr Polym Lett 2010, 4, 26.
9. Petersen, K.; Nielsen, P.; Olsen, M. Starch 2001, 53, 356.
10. Bastioli, C. Starch 2001, 53, 351.
11. Wu, C. S. Macromol Biosci 2008, 8, 560.
12. Marchessault, R. H.; Morehead, F. F.; Koch, M. J. J Colloid Sci 1961, 16, 327.
13. Yao, S. J. Chin J Chem Eng 1999, 7, 47.
14. Araki, J.; Wada, M.; Kuga, S. Langmuir 2001, 17, 21.

15. Qu, P.; Gao, Y.; Wu, G. F.; Zhang, L. P. BioResources 2010, 5, 1811.
16. Nair, K. G.; Dufresne, A.; Gandini, A.; Belgacem, M. N. Biomacromolecules 2003, 4, 1835.
17. Ljungberg, N.; Bonini, C.; Bortolussi, F.; Boisson, C.; Heux, L.; Cavaille, J. Biomacromolecules 2005, 6, 2732.
18. Goussé, C.; Chanzy, H.; Cerrada, M. L.; Fleury, E. Polymer 2004, 45, 1569.
19. Lin, N.; Chen, G. J.; Huang, J.; Dufresne, A.; Chang, P. R. J Appl Polym Sci 2009, 113, 3417.
20. Goussé, C.; Chanzy, H.; Excoffier, G.; Soubeyrand, L.; Fleury, E. Polymer 2002, 43, 2645.
21. Lu, J.; Askeland, P.; Drzal, L. T. Polymer 2008, 49, 1285.
22. Chiang, C. H.; Ishida, H.; Koenig, J. L. J Colloid Interf Sci 1980, 74, 396.
23. Abdelmouleh, M.; Boufi, S.; Belgacem, M. N.; Duarte, A. P.; Ben Salah, A.; Gandini, A. Int J Adhes Adhes 2004, 24, 43.
24. Stiubianu, G.; Racles, C.; Cazacu, M.; Simionescu, B. C. J Mater Sci 2010, 45, 4141.
25. Ljungberg, N.; Cavaillé, J. Y.; Heux, L. Polymer 2006, 47, 6285.
26. Suarez, J. C. M.; Coutinho, F. M. B.; Sydenstricker, T. H. Polym Test 2003, 22, 819.